JACS
JOURNAL OF THE AMERICAN CHEMICAL SOCIETY
Article
pubs.acs.org/JACS

Catalyst Chemical State during CO Oxidation Reaction on Cu(111) Studied with Ambient-Pressure X-ray Photoelectron Spectroscopy and Near Edge X-ray Adsorption Fine Structure Spectroscopy

Baran Eren,[†] Christian Heine,[†] Hendrik Bluhm,[‡] Gabor A. Somorjai,[§] and Miquel Salmeron*[,†,∥]

[†]Materials Division and [‡]Chemical Sciences Division, Lawrence Berkeley National Laboratory, 1 Cyclotron Road, Berkeley, California 94720, United States

[§]Department of Chemistry, University of California, Berkeley, California 94720, United States

[∥]Department of Materials Science and Engineering, University of California, Berkeley, California 94720, United States

Supporting Information

ABSTRACT: The chemical structure of a Cu(111) model catalyst during the CO oxidation reaction in the CO+O_2 pressure range of 10−300 mTorr at 298−413 K was studied *in situ* using surface sensitive X-ray photoelectron and adsorption spectroscopy techniques [X-ray photoelectron spectroscopy (XPS) and near edge X-ray adsorption fine structure spectroscopy (NEXAFS)]. For O_2:CO partial pressure ratios below 1:3, the surface is covered by chemisorbed O and by a thin (∼1 nm) Cu_2O layer, which covers completely the surface for ratios above 1:3 between 333 and 413 K. The Cu_2O film increases in thickness and exceeds the escape depth (∼3−4 nm) of the XPS and NEXAFS photoelectrons used for analysis at 413 K. No CuO formation was detected under the reaction conditions used in this work. The main reaction intermediate was found to be $CO_2^{\delta-}$, with a coverage that correlates with the amount of Cu_2O, suggesting that this phase is the most active for CO oxidation.

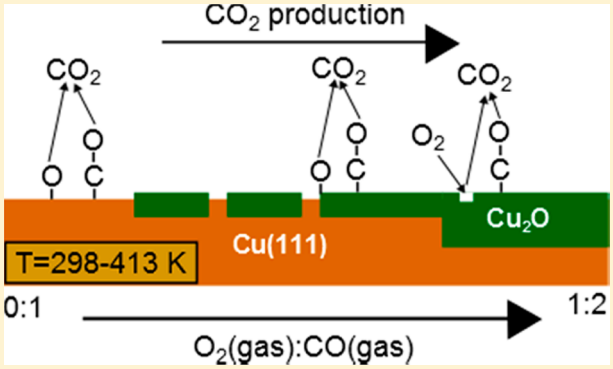

1. INTRODUCTION

CO oxidation is a prototypical reaction for fundamental studies and provides insights into more complicated reactions such as the water−gas shift or methanol oxidation.[1] Therefore, the CO oxidation reaction on model Cu catalysts (single-crystal Cu surfaces, thin Cu films, and Cu powders) has been investigated in various laboratories over recent decades.[2−7] Although Cu-based materials are common heterogeneous catalysts used in industry for water−gas shift, methanol oxidation, and methanol synthesis reactions,[8−14] they suffer from a swift deactivation during CO oxidation.[15] A major roadblock in understanding the reaction is the unknown chemical state of the catalyst during reaction, although it has been assumed to be a mixture of Cu, Cu_2O, and CuO, the latter assumed to deactivate the surface.[15] The unknown nature of the most active catalyst state, Cu or Cu_2O, remains an open question as reflected in the disagreements persisting in the literature to this day.[4−6,15] A surface science study on a well-defined surface and under well-defined reaction conditions is therefore of utmost importance to clarify some of the uncertainties.

Direct access to the nature and coverage of adsorbed species (both reactants and reaction intermediates) as well as to the chemical state of the catalyst surface and subsurface during reaction has become possible in the past decade thanks to the development of ambient-pressure (AP) X-ray spectroscopy techniques, especially X-ray photoelectron spectroscopy (XPS) and near edge X-ray adsorption fine structure spectroscopy (NEXAFS).[16,17] In the study presented here, both the chemical state of the catalyst and the relative coverage of adsorbed species (CO, O, and $CO_2^{\delta-}$) are identified at reactant pressures of a few tenths of Torr between 298 and 413 K using these techniques. Copper single-crystal surfaces are chosen to eliminate the effects of grain boundaries, which are known to facilitate the formation of subsurface oxygen.[18,19] Recent scanning tunneling microscopy (STM) studies have shown that the presence of gas phase CO in the pressure range of 0.2−1 Torr results in the breakup of the (111) surface into two-dimensional clusters.[20] Similarly, in the presence of a few millitorr of oxygen, a rough oxide is formed on the surface.[6] Here we show that while Cu easily oxidizes to Cu_2O, further oxidation to CuO does not take place under our reaction conditions. The main reaction intermediate is found to be $CO_2^{\delta-}$, present with a coverage that correlates with the amount of Cu_2O, suggesting that this phase is the most active for CO oxidation.

Received: July 16, 2015
Published: August 14, 2015

DOI: 10.1021/jacs.5b07451
J. Am. Chem. Soc. 2015, 137, 11186−11190

2. EXPERIMENTAL SECTION

The single-crystal preparation and characterization experiments were performed at a base pressure in the low 10^{-10} Torr range, at beamline 11.0.2 of the Advanced Light Source, the Berkeley synchrotron facility. The Cu(111) surface was cleaned by sputtering (5 min at 1×10^{-5} Torr of Ar, 1 keV) and annealing (15 min at 823 K) cycles, until no peaks other than those of Cu were detected by XPS. After preparation, CO gas was leaked into the chamber after being passed through a carbonyl trap at 513 K. The total pressure was measured with a MKS 722A Baratron capacitance pressure gauge. During each experiment, the temperature was fixed (298, 333, 373, or 413 K), and AP-XPS and AP-NEXAFS data were collected, first in ultrahigh vacuum (UHV), then in 0.3 Torr of CO and 0−0.15 Torr of O_2, and again in 0.3 Torr of CO after the O_2 had been pumped out. Finally, additional spectra were obtained in UHV after CO had been pumped out. The O_2:CO partial pressure ratios were selected as 3:97, 1:10, 1:3, and 1:2.

Photon energies (E_{ph}) of 1150 eV for Cu 2p, 490 eV for C 1s, and 735 eV for O 1s were used to produce photoelectrons with kinetic energies (E_{kin}) of ∼200 eV for the APXPS measurements. The peak positions were referred to the Fermi level, measured in the same spectrum at the corresponding photon energy. Peak areas and widths were measured from Doniac−Sunjic fits of the spectra. Furthermore, O 1s spectra with an E_{ph} of 1150 eV and C 1s spectra with an E_{ph} of 900 eV were also measured to obtain information from greater sampling depths.

The NEXAFS measurements in the O K and Cu $L_{2,3}$ edges were performed in the Auger-Meitner Electron Yield (AMEY) mode. With an analyzer pass energy of 50 eV, the retarding field was chosen to collect electrons with an E_{kin} of 300 eV to suppress contributions from the gas phase, as reported in ref 21. The photon energy was varied with a step size of 0.2 eV, between 520 and 560 eV for the O K edge, and between 920 and 960 eV for the Cu $L_{2,3}$ edges. The differences between the measured position of the π^* resonance of CO (533.9 eV) and O_2 (530.8 eV) and the literature values (534.1 eV for CO and 530.8 eV for O_2)[22] are within the experimental error. In the case of the Cu $L_{2,3}$ edge, reference spectra of pure Cu and Cu_2O were measured, both showing a strong resonance at 933.2 eV. Literature values for these resonances were reported to be 933.7 eV,[23] indicating that the error in the absolute value is ∼0.5 eV.

All of the collected APXPS and AP-NEXAFS spectra are presented in the Supporting Information.

3. ANALYSIS AND INTERPRETATION OF XPS AND NEXAFS SPECTRA

Because determination of the catalyst structure and composition and that of the adsorbed species is crucially dependent on the interpretation of XPS and NEXAFS data, we proceed here to analyze these spectra and the origin and assignment of the various peaks.

Apart from oxygen bound in molecules in the gas phase (CO, O_2, and CO_2) or adsorbed on the surface (CO and $CO_2^{\delta-}$), which produce XPS peaks at higher binding energies, we distinguish different types of O bound to Cu atoms, which are the ones that characterize the catalyst chemical state. They all produce XPS peaks at lower binding energies. The first is chemisorbed oxygen, usually in the form of ordered mono- or submonolayers. Other types of oxygen are in oxide structures such as Cu_2O and CuO. These oxides should have a minimal thickness equal to one unit cell of the corresponding crystal. Finally, we can also have dissolved O atoms, occupying tetrahedral or octahedral sites deeper in the subsurface region.

3.1. XPS. Figure 1 shows O 1s and C 1s XPS as well NEXAFS O K edge and Cu L_3 edge spectra measured at various gas phase O_2:CO ratios.

The peak at 529.4 eV corresponds to O chemisorbed on the Cu(111) surface, as shown in previous studies.[7,23,24] In addition

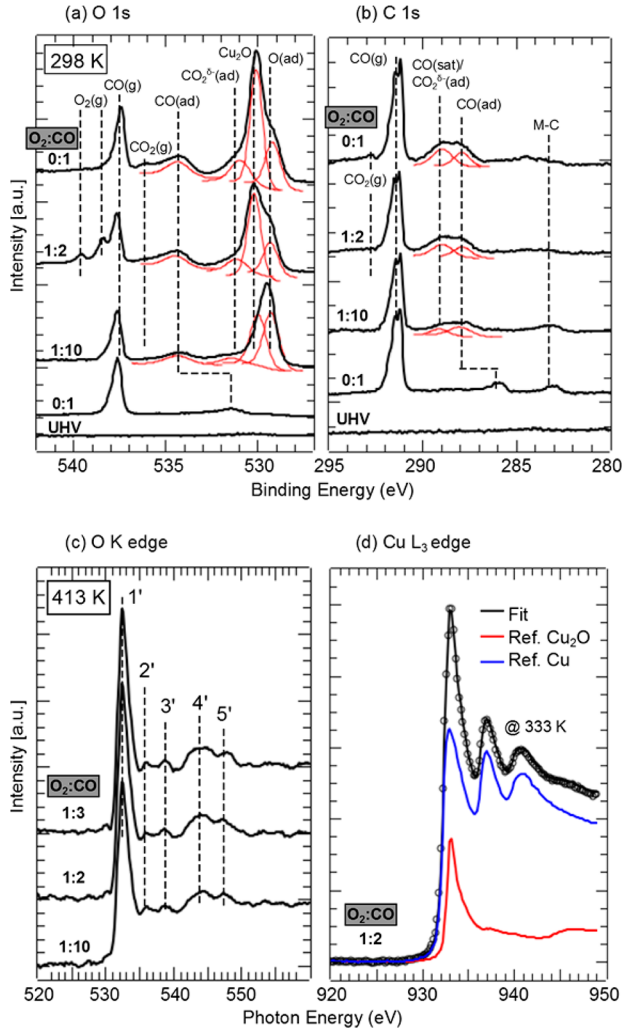

Figure 1. (a and b) Examples of APXPS O 1s and C 1s spectra from a Cu(111) sample at 298 K: in UHV, under 0.3 Torr of CO, under 0.03 Torr of O_2 and 0.3 Torr of CO, under 0.15 Torr of O_2 and 0.3 Torr of CO, and after pumping the O_2 (from bottom to top, respectively). The gas phase CO, O_2, and CO_2 peaks appear at binding energies higher than 536 eV in the O 1s region and higher than 290 eV at the C 1s region. Peaks arising from molecularly adsorbed CO are observed at 531.5 and 286.1 eV on metallic Cu and around 534.2, 287.9, and 289 eV (satellite) on the CuO_2-covered region. The chemisorbed O peak produced a peak at 529.4 eV both on the metallic Cu and on Cu_2O. The lattice O from Cu_2O appears at 530.2 eV. Adsorbed $CO_2^{\delta-}$, intermediate of the CO oxidation reaction, occurs at 531.5 and 289 eV. Small amounts of CH_x (284.4 eV) and carbon (M-C, 283.1 eV) are observed sometimes when O_2 is absent from the gas phase, because of beam-induced dissociation of CO. (c and d) AP-NEXAFS spectra at the O K and Cu L_3 edges. The O K edge has five different resonance peaks (1′−5′) originating from Cu_2O. (d) Reference Cu and Cu_2O spectra (bottom curves) and example of a spectrum from a partially oxidized sample (○). Its spectrum can be fitted by a linear combination of the pure Cu and Cu_2O spectra.

to the chemisorbed layer, a new peak grows with increasing exposure to O_2 at 530.2 eV, which we assign to formation of Cu_2O.[23,25] However, the peak at 529.4 eV still exists even after a surface oxide layer has fully formed (shown later). Although O from CuO was also reported to appear at 529.4 eV in the literature,[23] we can rule out this possibility here because the full width at half-maximum and the asymmetry parameter of the Sonjac−Dunjic functions of the Cu 2p peaks remained

DOI: 10.1021/jacs.5b07451
J. Am. Chem. Soc. 2015, 137, 11186−11190

unchanged (all Cu 2p spectra collected are shown in section 2.1.3 of the Supporting Information). The CuO phase is typically observed to produce Cu 2p peaks at an energy 1.4 eV higher than those of Cu and Cu_2O, which would have resulted in a shoulder (or a change in the asymmetry parameter) and satellite peaks at higher binding energies. Subsurface O is also unlikely the cause of the 529.4 eV peak because the intensity ratio between this peak and that at 530.2 eV is significantly lower at E_{ph} = 1150 eV than at E_{ph} = 735 eV. The peak at 529.4 eV was always observed in the reference O 1s spectra of pure Cu_2O.[23,26] Therefore, we attribute this peak to O adsorbed on defect sites (e.g., step edges and domain boundaries) of the Cu_2O layer. A peak with a similar energy was previously attributed to O adsorbed on defect sites of Cu(110) during the methanol oxidation reaction.[27] To further confirm our assignment, 0.1 Torr of oxygen was dosed onto a bulk Cu_2O sample, which resulted in very significant increase in the 529.4 eV peak with no CuO formation (confirmed with Cu 2p peaks). In summary, the peak at 529.4 eV in the study presented here can originate from chemisorbed O on metallic Cu or from O adsorbed on defect sites of Cu_2O.

The gas phase peaks of CO, O_2, and CO_2 (the latter as a reaction product) appear above 536 eV in the O 1s region and above 289 eV in the C 1s region. The peaks at around 531.5 and 286.1 eV arise from CO adsorbed on metallic Cu(111).[7] The reaction intermediate ($CO_2^{\delta-}$) was reported in the literature to produce O and C peaks at 531.4 and 288.4 eV on metallic Cu;[26,28] however, there is a lack of data about the $CO_2^{\delta-}$ and CO peak energies on Cu_2O. Here we assign the peaks at around 531.5 and 289.0 eV to $CO_2^{\delta-}$ on Cu_2O and the peaks at around 534.2 and 287.9 eV to CO on Cu_2O. We did not observe any carbonate peaks at 531.9 or 289.3 eV.[29] To confirm our peak assignments, a reference bulk Cu_2O sample was prepared and CO and CO_2 adsorption experiments were performed at room temperature (under 0.1 Torr of CO and under 0.4 Torr of CO_2). The peaks arising from CO and $CO_2^{\delta-}$ were indeed found at the aforementioned positions. However, CO adsorption on Cu_2O also resulted in an intense satellite peak at 289 eV similar to intense satellites in CO adsorbed on metallic Cu.[7,30] During our reaction studies, the peaks at 531.5 and 534.2 eV had intensities lower than that of the oxide peak (530.2 eV) at E_{ph} = 1150 eV than at E_{ph} = 735 eV, confirming that these are indeed surface species. The same is also true for the C 1s spectra. All the O 1s spectra collected at E_{ph} = 735 eV and E_{ph} = 1150 eV are shown in sections 2.1.1 and 2.2.1 of the Supporting Information. Similarly, all the C 1s spectra collected at E_{ph} = 490 eV and E_{ph} = 900 eV are shown in sections 2.1.2 and 2.2.2 of the Supporting Information.

Finally, the possible effect of water impurities in the chamber was assessed by dosing 0.05 Torr of H_2O on Cu_2O, which produced a peak at 531.3 eV due to formation of OH. This peak has a position very similar to that of the peak arising from $CO_2^{\delta-}$ adsorption.

3.2. NEXAFS. Figure 1c shows the O K edge NEXAFS spectra collected at 413 K at various O_2/CO gas pressures. The spectra contain the characteristic five resonances of Cu_2O:[31,32] 1′ at 532.4 eV and 2′ from 535.7 eV both arising from the O 2p Cu 3p hybridization, 3′ at 538.7 eV arising from the O 2p Cu 4sp hybridization, 4′ at 544.5 eV arising from the O 2p Cu 4sp4d hybridization, and 5′ at 548.1 eV arising from the O 2p3d Cu 4p4d hybridization. The energies of these resonances match recent theoretical calculations of the spectra.[23] The ratio between the intensities of the resonances depends on the stoichiometry, as discussed in section 5 of the Supporting Information. Chemisorbed oxygen on Cu was shown to produce a π^* resonance peak at around 530 eV and a broad peak at 533.6 eV.[22] Therefore, we attribute the small peak at 530.1 eV, which is prominent at 298 and 333 K, to the O 2p Cu 3p hybridization involving chemisorbed oxygen. This was confirmed with a reference oxygen adsorption experiment with Cu_2O. The existence of the peak at 530.1 eV at the O K edge is in line with the presence of the XPS peak at 529.4 eV from surface oxygen, even after the surface is fully oxidized to Cu_2O. We did not observe a clear peak from CO or $CO_2^{\delta-}$ in the O K edge spectra during CO and CO_2 adsorption experiments on Cu_2O at room temperature. This is because of low CO and $CO_2^{\delta-}$ coverage, low photon flux at E_{ph} = 530 eV, and the fact that only around 18% of the total intensity originates from the first layer for E_{kin} = 530 eV, whereas around 30% originates from surface species for E_{kin} = 200 eV.

Figure 1d shows the Cu L_3 edge NEXAFS spectra of pure Cu and Cu_2O phases, which were used as references to determine the ratio of metallic copper and Cu_2O concentrations, within the inelastic mean free path (IMFP ∼ 1.5−1.7 nm) of the 930 eV electrons used in the AMEY measurements. A linear fit of the pre-edge region between 920 and 928 eV was used for background subtraction. After this, the Cu L_3 edge was normalized with respect to the area (920−949 eV). The top curve is an example of a spectrum collected under reaction conditions. The spectrum can be explained as a superposition of the two reference spectra, with the components indicating the atomic ratio between the Cu and Cu_2O phases. All Cu $L_{2,3}$ edge spectra are shown in section 3.1 of the Supporting Information.

4. EVOLUTION OF THE CATALYST SURFACE AND SUBSURFACE DURING REACTION

In the following, the ratio of the XPS O 1s peak at 530.2 eV (oxide peak) to the Cu 2p peak (shown in section 2.1.3 of the Supporting Information) calibrated from a reference bulk Cu_2O sample, and the NEXAFS Cu L_3 edge, were used to calculate the chemical composition of the catalyst surface and near-surface region during the CO oxidation reaction. The O 1s peak is sensitive to the first one to four layers because the IMPF of the collected electrons is around 0.87 nm at E_{kin} = 200 eV, whereas the Cu L_3 is sensitive to the first one to eight layers because the Auger electrons (E_{kin} = 930 eV) have an IMPF of 1.46 nm for Cu and an IMPF of 1.73 nm for Cu_2O.[33]

The left panel of Figure 2 shows the evolution of the O:Cu atomic concentration ratio as a function of the O_2:CO pressure ratio. Above 333 K, more than 85% of the surface is oxidized to Cu_2O for a O_2:CO partial pressure ratio of 1:3. An important result is that after O_2 is pumped out of the chamber and only CO is maintained, no significant reduction from Cu_2O to Cu can be observed during our experimental time (≥0.5 h), at least for ≤413 K.

The right panel of Figure 2 shows a similar plot of the chemical state of the catalyst, this time calculated from NEXAFS fits such as those shown in Figure 1d. Because the NEXAFS data were acquired by collecting 930 eV AMEY electrons, it reflects the average composition of a slab of the surface ∼1.7 nm thick, which includes both the top Cu_2O layer that fills the 0.86 nm depth detected by XPS in the left panel and an additional subsurface contribution from the remaining thickness down to 1.7 nm. As we can see for O_2:CO partial pressure ratios above 0.3, more than 70% of the near-surface

DOI: 10.1021/jacs.5b07451
J. Am. Chem. Soc. 2015, 137, 11186−11190

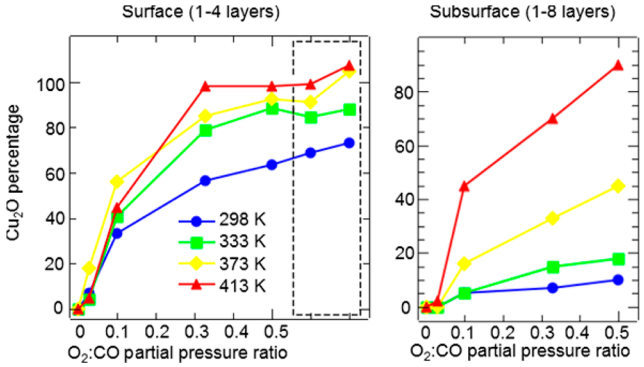

Figure 2. Cu_2O percentage (rest is metallic Cu) of the surface estimated from the intensity ratio between O 1s (530.2 eV) and Cu 2p XPS peaks (left). Cu_2O percentage (rest is metallic Cu) on the near-surface region estimated from the NEXAFS resonance at the Cu L_3 edge (right). Data are shown as a function of O_2:CO partial pressure ratio and temperature. The two data points inside the dashed box indicate points at which O_2 is pumped out (first data point, with CO still remaining in the chamber) and after CO is pumped out (second data point).

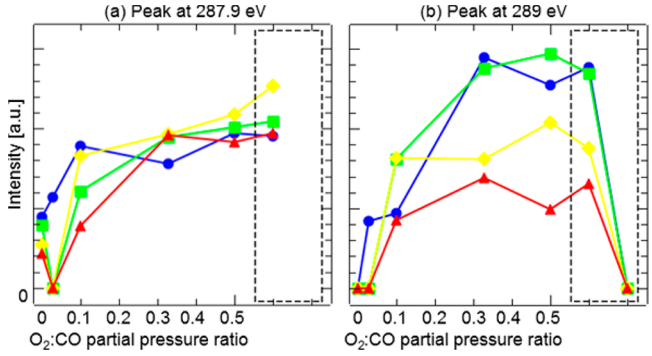

Figure 4. Relative intensities of the APXPS peaks (a) at 287.9 eV produced by molecularly adsorbed CO and (b) at 289 eV produced by both molecularly adsorbed CO and $CO_2^{\delta-}$ (reaction intermediate) as a function of O_2:CO partial pressure ratio and temperature. The two data points inside the dashed box are taken after O_2 is pumped out (with CO still remaining in the chamber; first data point) and after CO is pumped down (second data point).

region down to 1.7 nm is oxidized to Cu_2O at 413 K, while at ≤373 K, only the first 0.86 nm contains Cu_2O, the rest being mostly metallic Cu. Of course, the transition between Cu_2O and metallic Cu is not likely to be abrupt, but we do not have enough data to construct an O concentration profile at present.

5. REACTION MECHANISM

The coverages of adsorbed reactants (CO and O) and the $CO_2^{\delta-}$ reaction intermediate were followed from the O 1s and C 1s XPS intensities, as in the example shown in panels a and b of Figure 1. Figures 3 and 4 show the coverages of these three species as a function of O_2:CO pressure ratio. The observed evolution is strongly correlated to Cu_2O formation. As can be seen, when the catalyst is covered by Cu_2O layers, at a O_2:CO pressure ratio above 0.3, the coverage of the two reactant molecules is comparable.

The $CO_2^{\delta-}$ intermediate appears on the surface in amounts that follow the coverage of Cu_2O. This does not originate from a higher $CO_2^{\delta-}$ binding energy on Cu_2O than on Cu, because we measured ∼1.5 times higher $CO_2^{\delta-}$ coverage on Cu than on Cu_2O during adsorption experiments in the presence of 0.4 Torr of CO_2 at 298 K, which implies that while smaller, the binding energy on Cu_2O is still sufficiently high to maintain the observed coverage. This leaves a higher rate of CO_2 production on Cu_2O as the most likely explanation. The fact that nearly no CO is adsorbed on the surface under oxygen-lean conditions indicates also that the CO + O → CO_2 reaction takes place on Cu_2O rather than on metallic Cu. The chemisorbed and/or lattice oxygen in Cu_2O consumed by the reaction is replenished via dissociative O_2 adsorption.

It is remarkable that no rapid reduction of the Cu_2O to Cu was observed even at 413 K under 0.3 Torr of CO when the O_2 was removed from the chamber, even as the reaction continued to proceed, as shown by the presence of $CO_2^{\delta-}$. This was previously rationalized by replenishment from subsurface O.[15,18,19] A similar phenomenon was also proposed for Pd catalysts during CO oxidation reaction, which requires a thin oxide film for high catalytic activity.[34] The results presented

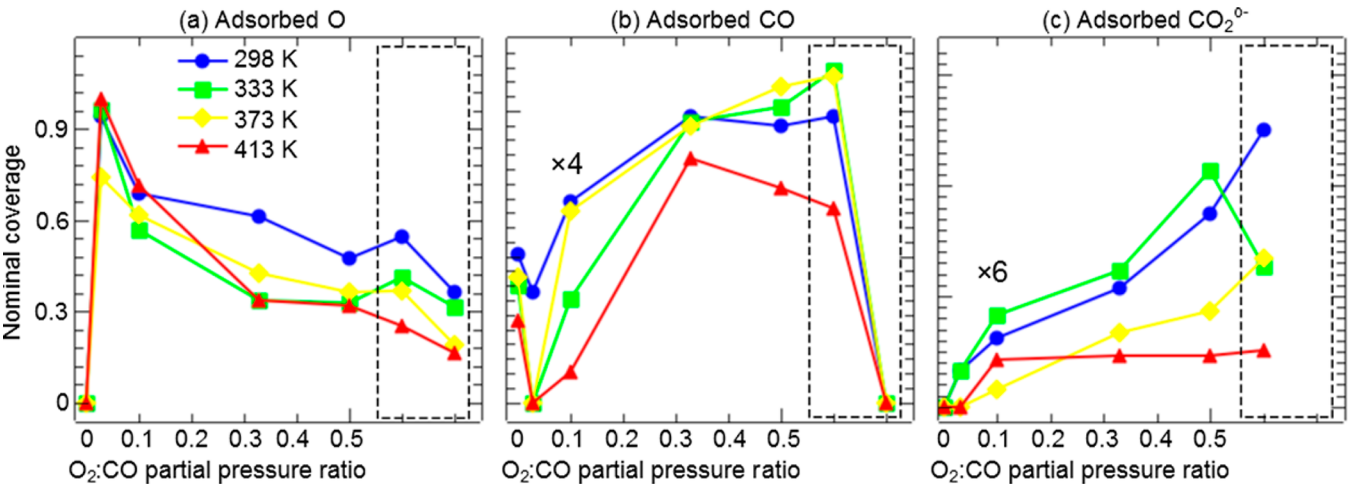

Figure 3. Coverage (±20%) of adsorbed species with respect to a flat Cu(111) surface as a function of O_2:CO partial pressure ratio and temperature calculated from the corresponding O 1s APXPS peaks: (a) dissociatively adsorbed oxygen, (b) molecularly adsorbed CO, and (c) $CO_2^{\delta-}$ (reaction intermediate). The peak intensity ratios are calibrated using intensity ratios of samples with known coverages.[7] The last two data points in the dashed box are taken after O_2 is pumped out (with CO remaining in the chamber) and after CO is pumped out, respectively.

DOI: 10.1021/jacs.5b07451
J. Am. Chem. Soc. 2015, 137, 11186−11190

here could indeed be interpreted in this way, because although no XPS peak due to oxygen dissolved in the Cu matrix could be detected due to a small photoemission cross section, a small photon flux, and a low concentration, the rate of diffusion to the surface could still be high enough to replenish the vacancies.

At present, our results cannot distinguish between a Mars van-Krevelen type mechanism involving reaction with lattice O from a Langmuir−Hinshelwood mechanism involving CO and O bound to surface Cu^+ defects on Cu_2O.

6. CONCLUSIONS

We have presented an *in situ* spectroscopic study of the chemical structure and evolution of a Cu(111) model catalyst during the CO oxidation reaction in the pressure range of 10−300 mTorr at 298−413 K. We found that under these conditions the catalyst surface during reaction was composed of Cu and/or Cu_2O depending on the oxygen partial pressure and temperature. The main highlights of this work can be summarized as follows. (1) CuO was not observed under the conditions of this work. (2) Under oxygen-lean conditions, the surface is not fully oxidized to Cu_2O. However, the surface is more reactive once a partial surface Cu_2O layer forms. (3) The surface coverage of CO is higher on Cu_2O than on metallic Cu, implying a higher CO adsorption energy on Cu_2O than on Cu. This is a favorable situation because the metallic Cu surface suffers oxygen poisoning because of the significant difference between CO and O adsorption energies, i.e., Sabatier effect.[7]

■ ASSOCIATED CONTENT

Supporting Information

The Supporting Information is available free of charge on the ACS Publications website at DOI: 10.1021/jacs.5b07451.

All the XPS (including Auger lines) and NEXAFS spectra, XPS intensity calibration, and more information about the NEXAFS O K edge (PDF)

■ AUTHOR INFORMATION

Corresponding Author

*mbsalmeron@lbl.gov

Notes

The authors declare no competing financial interest.

■ ACKNOWLEDGMENTS

This work was supported by the Office of Basic Energy Sciences (BES), Division of Materials Sciences and Engineering, of the U.S. Department of Energy (DOE) via Contract DE-AC02-05CH11231, through the Chemical and Mechanical Properties of Surfaces, Interfaces and Nanostructures program. H.B. acknowledges support from the Office of BES, Division of Chemical Sciences, Geosciences and Biosciences, of the U.S. DOE.

■ REFERENCES

(1) Freund, H.-J.; Meijer, G.; Scheffler, M.; Schlögl, R.; Wolf, M. *Angew. Chem., Int. Ed.* **2011**, *50*, 10064−10094.
(2) Szanyi, J.; Wayne Goodman, D. W. *Catal. Lett.* **1993**, *21*, 165−174.
(3) Domagala, M. E.; Campbell, C. T. *Catal. Lett.* **1991**, *9*, 65−70.
(4) Jernigan, G. G.; Somorjai, G. A. *J. Catal.* **1994**, *147*, 567−577.
(5) Huang, T.-J.; Tsai, D.-H. *Catal. Lett.* **2003**, *87*, 173−178.
(6) Xu, F.; Mudiyanselage, K.; Baber, A. E.; Soldemo, M.; Weissenrieder, J.; White, M. G.; Stacchiola, D. J. *J. Phys. Chem. C* **2014**, *118*, 15902−15909.
(7) Eren, B.; Lichtenstein, L.; Wu, C. H.; Bluhm, H.; Somorjai, G. A.; Salmeron, M. *J. Phys. Chem. C* **2015**, *119*, 14669−14674.
(8) Klier, K. Methanol Synthesis. In *Advances in Catalysis*; Eley, D. D., Pines, H., Weisz, P. B., Eds.; Academic Press: San Diego, 1982; Vol. *31*, pp 243.
(9) Newsome, D. S. *Catal. Rev.: Sci. Eng.* **1980**, *21*, 275−318.
(10) Szanyi, J.; Goodman, D. W. *Catal. Lett.* **1991**, *10*, 383−390.
(11) Yoshihara, J.; Campbell, C. T. *J. Catal.* **1996**, *161*, 776−782.
(12) Behrens, M.; Studt, F.; Kasatkin, I.; Kühl, S.; Hävecker, M.; Abild-Pedersen, F.; Zander, S.; Girgsdies, F.; Kurr, P.; Kniep, B. L.; Tovar, M.; Fischer, R. W.; Nørskov, J. K.; Schlögl, R. *Science* **2012**, *336*, 893−897.
(13) Olah, G. A. *Angew. Chem., Int. Ed.* **2013**, *52*, 104−107.
(14) Behrens, M. *Angew. Chem., Int. Ed.* **2014**, *53*, 12022−12024.
(15) Royer, S.; Duprez, D. *ChemCatChem* **2011**, *3*, 24−65.
(16) Salmeron, M.; Schlögl, R. *Surf. Sci. Rep.* **2008**, *63*, 169−199.
(17) Salmeron, M. *MRS Bull.* **2013**, *38*, 650−667.
(18) Sadykov, V. A.; Tikhov, S. F.; Bulgakov, N. N.; Gerasev, A. P. *Catal. Today* **2009**, *144*, 324−333.
(19) Bluhm, H.; Hävercker, M.; Knop-Gericke, A.; Teschner, D.; Eleimenov, E.; Bukhtiyarov, V. I.; Ogletree, D. F.; Salmeron, M.; Schlögl, R. *J. Phys. Chem. B* **2004**, *108*, 14340−14347.
(20) Eren, B.; Zherebetskyy, D.; Patera, L. L.; Wu, C. H.; Africh, C.; Wang, L. W.; Somorjai, G. A.; Salmeron, M. Manuscript submitted for publication.
(21) Hävecker, M.; Cavalleri, M.; Herbert, R.; Follath, R.; Knop-Gericke, A.; Hess, C.; Hermann, K.; Schlögl, R. *Phys. Status Solidi B* **2009**, *246*, 1459−1469.
(22) Stöhr, J. *NEXAFS Spectroscopy*; Springer-Verlag: Berlin, 2003.
(23) Jiang, P.; Prendergast, D.; Borondics, F.; Porsgaard, S.; Giovanetti, L.; Pach, E.; Newberg, J.; Bluhm, H.; Besenbacher, F.; Salmeron, M. *J. Chem. Phys.* **2013**, *138*, 024704.
(24) Baber, A. E.; Xu, F.; Dvorak, F.; Mudiyanselage, K.; Soldemo, M.; Weissenrieder, J.; Senanayake, S. D.; Sadowski, J. T.; Rodriguez, J. A.; Matolin, V.; White, M. G.; Stacchiola, D. J. *J. Am. Chem. Soc.* **2013**, *135*, 16781−16784.
(25) Okada, M.; Vattuone, L.; Rocca, M.; Teraoka, Y. *J. Chem. Phys.* **2012**, *136*, 094704.
(26) Deng, X.; Verdaguer, A.; Herranz, H.; Weis, C.; Bluhm, H.; Salmeron, M. *Langmuir* **2008**, *24*, 9474−9478.
(27) Günther, S.; Zhou, L.; Imbihl, R.; Hävercker, M.; Knop-Gericke, A.; Kleimenov, E.; Schlögl, R. *J. Chem. Phys.* **2006**, *125*, 114709.
(28) Copperthwaite, R. G.; Davies, P. R.; Morris, M. A.; Roberts, M. W.; Ryder, R. A. *Catal. Lett.* **1988**, *1*, 11.
(29) Deng, X.; Verdaguer, A.; Herranz, T.; Weis, C.; Bluhm, H.; Salmeron, M. *Langmuir* **2008**, *24*, 9474−9478.
(30) Tillborg, H.; Nilsson, A.; Mårtensson, N. *J. Electron Spectrosc. Relat. Phenom.* **1993**, *62*, 73−93.
(31) Schedel-Niedrig, T.; Neisius, T.; Böttger, I.; Kitzelmann, E.; Weinberg, G.; Demuth, D.; Schlögl, R. *Phys. Chem. Chem. Phys.* **2000**, *2*, 2407−2417.
(32) Knop-Gericke, A.; Hävercker, M.; Schedel-Niedrig, T.; Schlögl, R. *Top. Catal.* **2001**, *15*, 27−34.
(33) Tanuma, S.; Powell, C. J.; Penn, D. R. *Surf. Interface Anal.* **1994**, *21*, 165−176.
(34) Zhang, F.; Li, T.; Pan, L.; Asthagiri, A.; Weaver, J. F. *Catal. Sci. Technol.* **2014**, *4*, 3826.

DOI: 10.1021/jacs.5b07451
J. Am. Chem. Soc. 2015, 137, 11186−11190